Computational analysis of on-line coupled ITP-CE

Marc Horner, Ph.D.

Fluent Inc.
1007 Church St. Suite 250, Evanston, IL, 60201, marc.horner@fluent.com

ABSTRACT

Coupling isotachophoresis (ITP) to capillary electrophoresis (CE) has many benefits, but also introduces non-idealities into the concentrated sample. These non-idealities arise because of the interaction between the sample in the main flow channel and the pool of leading electrolyte in the side-arm. A computational model of the switching process was developed using FIDAP (Fluent Inc., Lebanon, NH). This paper presents a qualitative look at the asymmetries that arise during the switching process. Additionally, a control mechanism based on the time-derivative of voltage is also presented. This provides the user with real-time detection of the sample band as it passes the side-arm, and a means for implementing an automated switching strategy.

Keywords: isotachophoresis, electrophoresis, lab-on-a-chip, numerical simulation, CFD

1 INTRODUCTION

Lab-on-a-chip (or simply lab chip) technologies combine a sequence of (bio)chemical analyses on a single miniaturized platform. The lab chip is comprised of a series of narrow channels ($10\mu m < W < 500\mu m$) for performing the analysis. The main advantages of lab chips over their macro-scale counterparts are smaller sample volumes requirements, faster analysis times, and ease of automation.

Lab chip applications include chemical and biological agent detection, DNA sequencing/analysis, and drug discovery, to name only a few. Lab chips also have great potential in the point-of-care diagnostics (POCD) industry. POCD speed the medical decision-making process by providing an almost instantaneous measurement at the patient's bedside. POCD are especially useful when frequent status reports are required, e.g. blood glucose monitors and urine drug screens. POCD also avoid the inherent drawbacks of a central laboratory, such as long wait times and sample handling errors.

The microfluidic process can be broken down into a number of sub-tasks, primarily: sample introduction, pre-concentration, fluid handling, mixing, reaction, purification, filtration, analysis, and detection. The pre-concentration step is becoming more important as the initial sample volume decreases to nanoliter levels (and even further). Sample stacking and isotachophoresis (ITP) are common pre-concentration techniques. Both are mobility-based separations that require a discontinuous buffer system, but ITP is preferred because of the the decreased diffusional effects inherent in the separation.

Translated literally, isotachophoresis means constant speed. The name was chosen because the end result is a series of stacked bands - which are zones of constant mobility - that migrate at the same speed once the system reaches steady-state. The electric field is constant within each band, resulting in a self-correction mechanism that maintains distinct boundaries between the mobility bands even in the presence of diffusion. This self-correction can be explained as follows: analyte present in a region of higher relative mobility experiences a lower electric field and therefore slows down until it is back in the proper mobility band, likewise analyte present in a region of lower relative mobility experiences a higher electric field and can migrate ahead to the correct band. This self-correction mechanism is the hallmark of ITP [1].

Replacing the trailing electrolyte with leading electrolyte switches the separation from an ITP-mode to capillary electrophoretic (CE) mode. An on-line direct injection method is required to make the switch to CE, often by switching the voltage drop from the trailing electrolyte pool to a second pool of leading electrolyte. Transient effects associated with switching from ITP to CE may degrade the quality of the flowing sample, however. This is because the pre-concentrated sample must pass a source of leading electrolyte before switching to CE, resulting in uncontrolled mixing of the sample with leading electrolyte and/or loss of sample to the leading electrolyte pool.

A number of experimental implementations of coupled ITP-CE are present in the literature, see [2], [3], [4] to name only a few. Developing a computational model of this process allows for a detailed analysis of sample loss and dispersion and also a deeper understanding of the factors affecting sample purity. This paper presents an investigation of such non-idealities and also elucidates a methodology for controlling the switching process based on measurable system parameters.

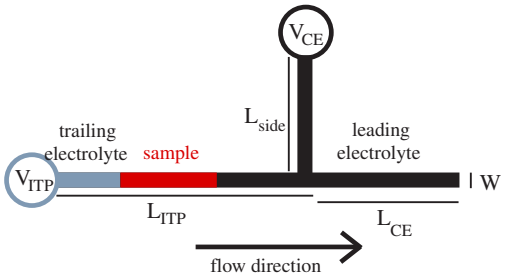

Figure 1: The 2-D microchannel geometry consists of a main channel and one side-arm. The electrolytes are initially arranged for ITP: the black area is filled with leading electrolyte, the red area with a mixture of two sample species, and the grey area with trailing electrolyte. L_{ITP} is the isotachophoretic zone and L_{CE} is the electrophoretic separation zone. The relevant dimensions are $L_{ITP} = 1500\ \mu$m, $L_{CE} = 1000\ \mu$m, $L_{side} = 500\ \mu$m, and $W = 50\ \mu$m.

2 PROBLEM DESCRIPTION

The prototypical T-junction geometry (figure 1) consists of a main channel and short side-arm. The main channel is divided into two separation zones: sample pre-concentration (ITP) occurs in the region before the side-arm and separation (CE) occurs in the region just past the side-arm. The side-arm is the source of leading electrolyte when switching from ITP to CE.

ITP requires a discontinuous buffer arrangement to pre-concentrate the analytes, each buffer having different electrophoretic mobilities (denoted b_i). The leading electrolyte has the highest mobility (b_L = 240.0E-5 cm^2/V-s) and the trailing electrolyte has the lowest mobility (b_T = 30.0E-5 cm^2/V-s) . The sample zone contains two species of intermediate mobility (b_1 = 120.0E-5 cm^2/V-s and b_2 = 30.0E-5 cm^2/V-s). Note that all ions have a charge of +1 except for analyte 2 which has a charge of +2, effectively doubling the mobility of this species. The permittivity (ϵ) is a function of the local species concentration,

$$\epsilon = \sum_i (z_i b_i c_i), \tag{1}$$

The diffusivity of all species is 1.0E-5 cm^2/s.

The initial concentration of leading and trailing electrolytes is 1.0, i.e. $c_{Lo} = c_{To} = 1.0$, and the initial concentration of the two sample analytes is $c_{1o} = c_{2o} = 0.2$. The two analytes will "adapt" to the concentration of the leading electrolyte during ITP, concentrating the analytes by a factor of five before heading in to the CE-phase. The well at location V_{ITP} is a continuous source of trailing electrolyte and the well at V_{CE} is a continuous source of leading electrolyte.

A step-change in the voltage is required to switch from ITP to CE. During ITP, the voltage drop across the main flow channel is 200 V/cm (V_{ITP} = 50 V) and a float condition is applied at the side-arm. Once the sample passes into the CE-zone, a voltage drop of 100 V/cm (V_{CE} = 15 V) is applied at the side-arm and the main channel inlet floats. The latter drives the flow of leading electrolyte from the side-arm into the main channel, and CE separation ensues because the sample is sandwiched between high mobility buffer solutions.

3 ELECTROHYDRODYNAMIC TRANSPORT EQUATIONS

The transport equations for electro-hydrodynamic flow are summarized in this section [5]. The Gauss law relation describes the distribution of the voltage (ϕ):

$$\nabla\cdot(\rho\epsilon\nabla\phi) = -\sum_i (\rho F z_i c_i), \tag{2}$$

where ϵ is the solution permittivity (defined in equation 1), ρ is the fluid density, F is the Faraday constant, and z_i and c_i are the charge and concentration of species i, respectively. Note that the electric field $E = -\nabla\phi$ and the local charge q is given by $\sum_i (F z_i c_i)$. Equation (2) is simultaneously coupled to the transport equations for species, momentum, and energy.

The conservation of species i is given by

$$\frac{\partial(\rho c_i)}{\partial t} + \nabla\cdot(\rho\mathbf{u}c_i) = \nabla\cdot(\rho D_i\nabla c_i) + \nabla\cdot(\rho z_i b_i c_i\nabla\phi) + R_i, \tag{3}$$

where D_i is the diffusivity of species i and R_i is the reaction rate of species i.

The Navier-Stokes equations describe the fluid flow,

$$\rho(\frac{\partial\mathbf{u}}{\partial t} + \mathbf{u}\cdot\nabla\mathbf{u}) = -\nabla P + \mu\nabla^2\mathbf{u} + q\mathbf{E}, \tag{4}$$

where $\mathbf{u} = u(x, y, z, t)$ is the fluid velocity, μ is the fluid viscosity, and P is the pressure. The Coulomb force term, $q\mathbf{E}$, represents the flow of fluid due to the motion of charged species. Equation (4) is constrained by the continuity equation, $\nabla\cdot\mathbf{u} = 0$.

Lastly, the energy equation is given by

$$\rho C_p(\frac{\partial T}{\partial t} + \mathbf{u}\cdot\nabla T) = k\nabla^2 T + \epsilon\mathbf{E}\cdot\mathbf{E}, \tag{5}$$

where T is temperature, C_p is the heat capacity, and k is the thermal conductivity. The last term in equation (5) represents the Joule heating effect. The primary consequence of this term is a radial temperature gradient across the capillary, which may decrease the resolution of the separation process.

3.1 Boundary conditions

The three forms of boundary conditions are Dirichlet, Neumann, and Robin. A Dirichlet condition specifies

the value of a given degree of freedom at a boundary, e.g. $\phi = K$, where K is typically a constant or a function of time. The Neumann condition specifies the diffusive flux,

$$(D\nabla c_i) \cdot \mathbf{n} = K, \tag{6}$$

and the Robin condition includes an electromigration (drift velocity) term in addition to the diffusive flux,

$$(D\nabla c_i + z_i b_i c_i \nabla \phi_i) \cdot \mathbf{n} = K. \tag{7}$$

Setting $K = 0$ in equation (6) permits an advective flux of ions through a boundary and/or transport via electromigration, while setting $K = 0$ in equation (7) permits advection only (for the case of small diffusive flux). Flux boundary conditions are typically used on the channel walls and/or the outlets of the channel network.

3.2 Numerical solution

The pre-processor GAMBIT (Fluent Inc., Lebanon, NH) was used to create the geometry and computational grid for the T-junction shown in figure 1. The mesh consists of linear, quadrilateral elements with a characteristic element size of 3 μm.

FIDAP (Fluent Inc., Lebanon, NH) was used to solve the system of EHD equations. FIDAP is a finite element code that uses a Galerkin formulation to discretize the steady-state form of each transport equation, and the backward Euler scheme for the time integration. A (low-memory) iterative solver was used to compute the transient results. The iterative solver solves for each degree of freedom independently, and then verifies global convergence, before proceeding to the next time-step.

A FORTRAN subroutine was required to calculate the permittivity (equation 1). This subroutine is accessed at the beginning of each iteration to calculate the permittivity for all nodes.

4 RESULTS

The results of an ITP-only simulation are discussed first and then compared to the simulation results for ITP-CE. The length of the ITP portion of the channel should be chosen such that the ITP separation is complete before the sample reaches the side-arm. This may be checked in the computational model by plotting the position of each mobility band and verifying that they are moving at a constant speed (figure 2*a*). Sharp boundaries between each mobility band should also persist as long as leading and trailing electrolyte are present (figure 2*b*).

Figure (3) illustrates the leakage of sample into the side-arm, and the resulting asymmetries in the sample plug advecting in the main channel (see figure 3*d*). Note that this leakage occurs in the ITP-mode, so some asymmetry and sample degradation are inherent in this type of switching methodology.

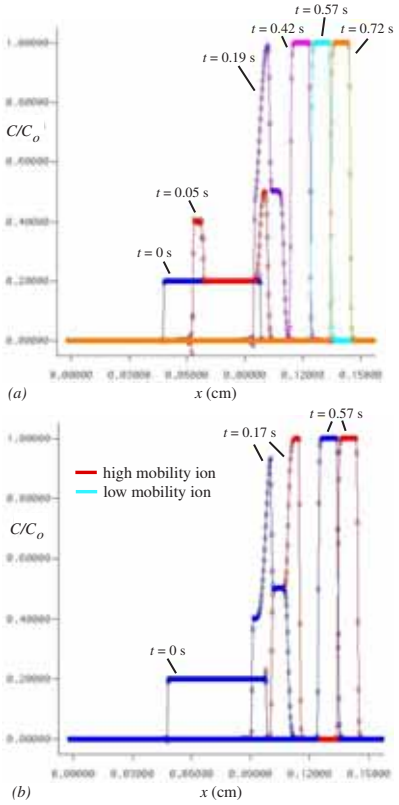

Figure 2: Isotachopherograms show the distribution of high and low mobility ions in the microchannel. These plots show that the isotachophoretic condition is satisfied before reaching the side-arm. Note that the concentration values were extracted along the center-line of the main flow channel.

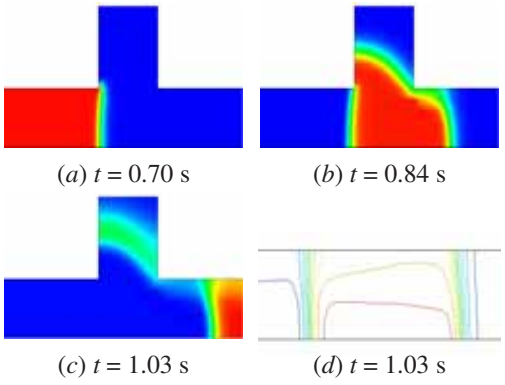

Figure 3: $(a-c)$ A portion of the sample remains in the side-arm even after the rest of the sample has separated from the downstream edge. (d) Concentration contours reveal asymmetries in the sample band. Note that red corresponds to a concentration of 1 and blue corresponds to concentration of 0.

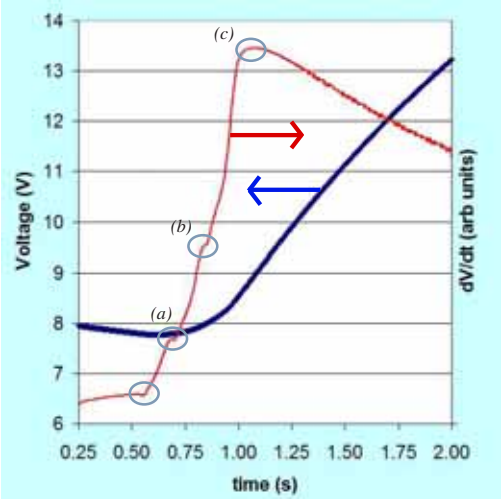

Figure 4: V and dV/dt as measured at a point in the center of the entrance of the side-arm. The points labelled $(a), (b)$, and (c) on the dV/dt curve correspond to the same time points shown in figure $3(a-c)$. Note that each hump corresponds to a distinct positioning "event", e.g. in (a) the hump occurs as the upstream portion of the sample arrives at the side-arm opening and (c) corresponds to the release of the sample from the side-arm.

It was also observed that the time-derivative of the voltage varies in a predictable way as each mobility band passes the side-arm (see figure 4). The figure shows small humps in dV/dt that are precisely timed with changes in the location of the sample band relative to the upstream and downstream edges of the side-arm. This behavior is a direct result of the sudden change in permittivity that occurs as each mobility band passes beneath the side-arm opening. The sharp interfaces between ITP bands means that this is a very precise measure of mobility band location.

Computational results for the case of coupled ITP-CE show significant differences from the ITP-only run. Figure (5) shows the location of the leading electrolyte and two sample species after the switch. Band-broadening is evident as is a decrease in the maximum analyte concentration. And concentration contours reveal that the switch leads to an increase in sample dispersion (figure 6). While this is expected in the longitudinal direction, there is also an increased concentration gradient across the channel width. A final important difference between ITP and ITP-CE is that the flow of leading electrolyte from the side-arm rapidly removes any residual analyte. Molecular diffusion is the only mechanism for removing analyte trapped in the side-arm when operating in the ITP-mode.

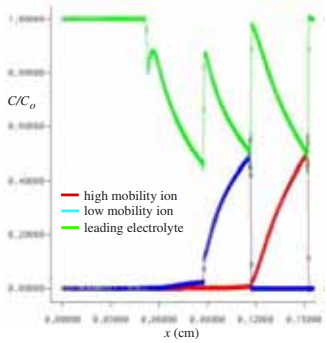

Figure 5: Isotachopherograms for the two analytes and leading electrolyte 0.17 s after the switch to CE. The analyte tails are longer while the fronts are still sharp.

Figure 6: Concentration contours for the low mobility ion 0.1 s after switching to the CE-mode. The switch induces even greater asymmetry in the sample versus ITP alone (compare to figure $3d$).

5 CONCLUSIONS

This paper summarizes a computational investigation of transient effects encountered during ITP and coupled ITP-CE. It was observed that interaction with a side-arm produces asymmetries in the concentrated sample, and the switch to CE magnifies these asymmetries. It was also observed that the time-derivative of voltage is a measurable parameter for controlling the switch to CE. The importance of this observation is that dV/dt is readily measured in an automated process. Changes are easily made to this model to optimize ITP-CE separations.

REFERENCES

[1] Everaerts, Beckers, and Verheggen, "Isotachophoresis, Theory, Instrumentation and Applications," Elsevier Scientific Publishing Company, 1976.

[2] C. Park, P. Kechagia, R.-L. Chien, and M. Spaid, 7th International Conference on Miniaturized Chemical and Biochemical Analysis Systems, October 5-9, 2003.

[3] L. Krivankova, P. Pantuckove, and P. Bocek, J. Chromatography A, 838, 55-70, 1999.

[4] W.N. Vreeland, S.J. Williams, A.E. Barron, and A.P. Sassi, Analyt Chem, 75, 3059-3065, 2003.

[5] FIDAP 8.5 Update Manual, Fluent Inc., Lebanon, NH, 2000.